RF Design and Predicted Performance for a Future 34-Meter Shaped Dual-Reflector Antenna System Using the Common Aperture X-S Feedhorn

W. F. Williams
Radio Frequency and Microwave Subsystems Section

The Networks Consolidation Program (NCP) will utilize 34-meter shaped dual-reflector Cassegrain antennas. This article discusses the shaping calculations, the X/S-band feedhorn to be used, and the predicted RF performance of this antenna system.

I. Introduction

The Networks Consolidation Program (NCP) will include at least two new 34-meter high-aperture-efficiency shaped dual-reflector antennas. This report presents the results of the geometric optics design which determines the dual reflector coordinates of the system and the calculated RF performance values of the antenna when using the recently developed DSN common aperture X-S feedhorn.

The functional requirement for the new NCP antennas is to provide a receive-only capability within modest bandwidths at X-band and S-band. However, there may be future requirements for uplink transmission in one or both bands because of anticipated new programs, e.g., the Galileo and other missions. To cover this eventuality, the microwave subsystem feedcones for the antennas were sized for various future expansions accommodating these potential transmit and other requirements. The microwave hardware, i.e., the feedhorn and S-band combiner, cannot easily be broad-banded and field retrofitted to include these additional functions. Therefore, since the expansions were anticipated, a basic transmit capability and other details have been engineered into the microwave subsystem. The expansion is fairly routine for the X-band portion of the horn alone, but the design for the broad-banding of the S-band injection was particularly vexing.

The objective of the 34-meter design was to maximize the gain/noise temperature (G/T) ratio of the antenna, the so-called figure of merit. A first step in achieving the maximum gain (high aperture efficiency) is to obtain a uniform illumination across the reflector aperture which maximizes illumination efficiency, while at the same time utilizing techniques which maximize all other efficiencies, i.e., reducing, to near elimination, forward spillover past the subreflector and reducing as best as possible the rear spillover (which significantly reduces system noise). This is best achieved (within the present state of the art) by using a specially shaped dual-reflector system. These special shapes are obtained by altering the hyperboloid contour so that the particular feedhorn pattern that is used will be transformed from a usual beam pattern to a basically uniform pattern when scattered from the altered subreflector. This is required for high main reflector illumination efficiency. This process is known to introduce illumination pattern phase departures from the spherical case; main reflector alteration is therefore employed to produce the final required phase uniformity.

The final shaping was determined using the X-band measured horn pattern (8.45 GHz) of the DSN developed X-S common aperture feedhorn. Final predicted values of RF performance were calculated by using the measured pattern data in X- and S-bands, and using theoretical predictions of the scattering from the subreflector. An attempt will be made to estimate certain RF efficiencies which are totally dependent upon mechanical design and construction. These will be the spar (quadripod) blockage efficiency and surface tolerance efficiency. Maximum and minimum values will be suggested for these efficiencies to permit the reader to place bounds on the estimates of final performance.

II. X-S Common Aperture Feedhorn and Combiner

In mid calendar year 1976 (early FY 77) a program was initiated to develop an S- and X-band feedhorn with objectives as follows:

(1) Obtain a centerline symmetric unit to replace present asymmetric simultaneous S/X reflex (dichroic plate) DSN feed systems and thereby

(2) Eliminate the dichroic plate and further optimize X-band performance, with degradation of S-band performance allowed if necessary, and

(3) Plan for the future capability of high power transmission in both X- and S-bands.

Shortly thereafter the present concept was conceived for the dual-band common aperture feedhorn. The major instigation for the concept was obtained from a paper by Jeuken and Vokurka (Ref. 1). In essence, that paper recalls that the corrugation depths for a corrugated horn need to be between $\lambda/4$ (λ = wavelength) and $\lambda/2$ to support the proper HE_{11} waveguide mode. It follows that any such corrugations would be odd multiples of these depths within certain other frequency bands as well. A careful choice of depth is then made to obtain operation within S-band and X-band with depths greater than $\lambda/4$ and less than $\lambda/2$ in S-band and greater than $5\lambda/4$ and less than $3\lambda/2$ in X-band. Thus a sort of "harmonic" operation of the corrugation depth is effected. As such a feedhorn with fixed flare angle is made longer, hence with larger aperture, a point is reached when further increase does not increase horn gain or reduce an associated beamwidth, e.g., 20 dB beamwidth. Details of pattern shape will differ with frequency, but not the gain or this beamwidth. One might call this "saturated gain" operation. Further detail of this approach may be found in Refs. 2 and 3.

As mentioned in the introduction, injecting or extracting S-band from this horn presented a major problem. A solution was found by feeding the horn at a sufficiently large horn diameter (above waveguide cutoff) region from a surrounding radial line which carries the S-band. S-band is injected into this radial line from four orthogonally located peripheral feed points excited in a 90° phase progression to develop circular polarization. The radial line carries two radial rejection chokes which prevents X-band from propagating within the S-band injection device, now termed the X/S-band combiner/separator. The system works very well in X-band since no noise temperature increase was noted when compared to the DSN standard X-band 22-dB horn, which has no S-band operation. The major shortcoming of the first generation combiner was its narrow S-band bandwidth, making it useful in a receive-only system. The problem has been overcome in a second generation combiner. This combiner is discussed in further detail in Ref. 4. A patent was issued for the horn combiner system (Ref. 5).

The final common aperture feedhorn and combiner for NCP is now complete. S-band bandwidth problems and a slight X-band moding problem were solved. Moding was better understood due to work by Thomas (Ref. 6), and the combiner frequency bandwidth was increased by increasing the height of the radial line. A paper (Ref. 7) has been presented which describes the techniques employed to achieve the final performance. A detailed description of the development with photographs and measured radiation patterns is given in Ref. 8. This reference details the predicted performance at DSS 13, using the 26-meter parabolic reflector. The microwave subsystem expansions envisioned for a "4-function feedcone," to cover anticipated future requirements as mentioned above, have already been largely incorporated, on an R&D basis, into the DSS-13 feedcone (Ref. 10). This feedcone is the first simultaneous dual-band receive/dual band transmit DSN system.

III. The Shaped Dual-Reflector System

Shaped dual-reflector antenna systems, sometimes called specially shaped Cassegrain antenna systems, have been in use for approximately 15 years. The first one to be placed in service was designed and built by the Philco-Ford Western Development Laboratory and located in Italy for the Intelsat service. This antenna had an aperture of 30 meters. Since that time a great many more antennas of varying sizes have been built by various companies and placed in service throughout the world.

The shaping consists of slight distortions of the usual hyperboloid subreflector of a Cassegrain system so that the feedhorn pattern can be transformed into a nearly uniform illumination across the main aperture. In so doing the uniform phase pat-

tern, normally present from the hyperboloid, is destroyed. This uniform phase is then recovered by slight (and similar) distortions of the usual paraboloid. The resulting uniform distribution of amplitude and phase gives the maximum possible illumination efficiency available from the given aperture size.

Since the shaping transforms a feedhorn pattern, it follows that a particular feedhorn pattern must be used to obtain the final reflector shape. Geometric optics is used to solve the problem, using only equal path lengths and Snell's law of reflection, so frequency of operation does not enter into the solution. Therefore, any feedhorn pattern at any frequency and reasonably uniform phase will be transformed to an illumination that will be distorted to an extent dependent upon the similarity of its pattern to the pattern that was used in basic shaping design. The geometric optics determined main reflector will then recover the uniform phase required for an antenna aperture. It must be mentioned that the standard paraboloid-hyperboloid Cassegrain system is only a special case of the general shaped dual-reflector antenna. In that case, the transformation is 1 to 1. That is, the feedhorn pattern is unchanged; the illumination becomes that of the feedhorn used in a prime focus system of greater focal length, modified slightly by finite reflector diffraction detail.

The JPL dual-reflector shaping software was prepared in about 1967 and, although exercised often, has never been used for the design of a system that was fabricated. Experimental or test designs of systems have been performed for comparison to the results as computed by two other organizations. The result has indicated that the JPL program compares very well and can be used with confidence.

A new feature has been added to the JPL program. (Ref. 3, p. 10.) This feature eliminates much of the illumination in the central region, hence reducing the subreflector blockage and improving blockage efficiency. Thus, the feature synthesizes what previously was termed a "vertex matching plate," but without an accompanying phase distortion.

As mentioned above, the common aperture feedhorn has been completed and the radiation patterns measured. The measured pattern at 8.450 GHz has been used to calculate the special shapes for the 34-meter NCP antennas. In performing this calculation, the distance from aperture plane to main reflector (quasi-paraboloid) vertex was chosen as a design parameter. This was done to match the 26-meter antennas of the DSN, and so the special shape solutions closely approximate the 26-meter paraboloid contour. The result was a feedhorn focal point location at 193.5 inches (4.915 meters) from the quasi-paraboloid vertex. Hence the new feedcone is compatible with any other DSN antenna for maximum flexibility.

Figure 1 is a control design outline drawing of the shaped antenna configuration. Note that the geometric ray from the quasi-hyperboloid edge does not go through the quasi-paraboloid edge, but instead intercepts at 645 inches (16.383 meters) from the Y-axis. The reason for this choice is as follows: The feedhorn scattered energy from the quasi-hyperboloid does not fall abruptly to zero at the angle θ_1 (Fig. 1), but instead tapers rapidly to a low level. The angle θ_1, and hence the 16.383-meter dimension, is chosen so that the intensity at θ_2 may be at a very low level relative to the central region of the main reflector, and the resulting rear spillover noise contribution becomes acceptably small. This results in a slightly lower illumination efficiency and hence antenna gain, but the significant reduction in noise from rear spillover allows an optimum G/T ratio.

Also note from Fig. 1 that an equivalent F/D is listed. It must be emphasized that this antenna has no unique focal length "F," but instead only a variable focus position which is a function of any particular ray from feed to subreflector to main reflector. The equivalent F/D is listed to serve as a description of the main reflector depth or the dimension from aperture to vertex for purposes of quick comparison to standard Cassegrain systems.

Complete Specification Control drawings for the dual-reflector system including coordinates of both reflectors are presented in JPL drawings 10097335 and 10097336.

As mentioned above, the shaping solution was performed to obtain a result that was a "best fit" to existing 26-meter paraboloid antennas. This was done so that individual 26-meter panels might be used to approximate the required shaped surface, hence potentially saving costs in the shaped surface fabrication. However, it was later decided to fabricate a complete new antenna structure with all new panels, but the original calculated contours have been retained.

IV. Predicted RF Feed System Performance of the New Antennas

The predictions of RF performance for the new NCP antennas were based upon the theoretical scattering (computer programs) of the measured common aperture X-S horn patterns from the shaped subreflector surface. Results will be presented for frequencies in both X- and S-band.

A JPL computer program has been prepared which calculates the efficiencies of a paraboloidal reflector system based upon its illumination pattern. All the calculated efficiencies remain the same for our quasi-paraboloid relative to a paraboloid system except for phase efficiency. As was mentioned earlier, the scatter pattern from the shaped subreflector has a

nonuniform phase function; the funtion of the quasi-paraboloid is to correct for this to obtain the necessary uniform phase front. This is the only function or purpose of the modification to the paraboloid. Therefore, another computer program has been prepared which performs this phase adjustment just as the quasi-paraboloid does. The illumination pattern for efficiency calculation then has the near uniform phase function, but normal feed phase variations and hence diffraction phase characteristics have been maintained. This phase corrected illumination pattern is then used in the efficiency program.

Figures 2, 3, 4 and 5 present subreflector scattered patterns of the measured feedhorn patterns at the four noted frequencies. Table 1 lists the resulting calculated efficiency elements comprising the RF feed system performance. An additional efficiency of 0.97 has been included to represent an estimate of dissipative loss and loss due to voltage standing wave ratio. It must be emphasized that no allowance has been made for the structural/mechanical losses mentioned above.

A noise level in kelvins (K) is listed beside values of rear spillover. This is an estimate of noise contribution from the spillover energy that will come from the earth source. The estimate is made as follows: (1.0 − η (rear spillover)) is the fractional noise energy from the earth that enters the antenna feed system and receiver. The estimate made is that the average blackbody radiation is such as to make the temperature 240 K, instead of the 300 K maximum. Therefore, 240 K is multiplied times this fraction to obtain values of temperature directly attributable to the "hot" earth.

It now becomes possible to maximize G/T for different aperture illumination angles, again considering only the RF feed system. These RF values will be reduced for a final estimate by the values of gain reduction attributable to surface tolerance and spar blockage. For the G/T estimate it is assumed that the noise from rear spillover is reduced by 50% at a 30-deg elevation angle since much less earth is then seen by the rear spillover. Table 2 presents the results of these calculations. This table shows the result of making the quasi-hyperboloid edge ray incident upon a point well within the quasi-paraboloid aperture edge, i.e., $\theta_2 > \theta_1$ (see Fig. 1). If the design were made so that $\theta_1 = \theta_2$ (ray from edge to edge) the rear spillover noise would be from 4 K to 8 K, a value large enough to significantly reduce G/T from the potential maximum. Figure 6 presents the information in graph form, indicating a region of optimum operation.

Final secondary patterns have also been calculated. This is done by using the phase altered scatter patterns of Figs. 2 and 4 as illumination functions for a true paraboloid. The paraboloid is chosen to have the same total illumination angle as the shaped system, i.e., 2 X 72.79 = 145.58 deg. These calculated patterns are depicted in Figs. 7 and 8. It must be pointed out that these are "best possible" patterns since neither surface tolerance nor spar blockage has been considered, and each will increase side lobe level and decrease gain somewhat. Beamwidth prediction should be quite close.

V. Final System Performance Based Upon Blockage and Surface Tolerance Assumptions

A short discussion of surface tolerance efficiency by Ruze and of JPL experience with spar blockage efficiency is given in Ref. 9. It will be the purpose of this final section to use extremes of both efficiencies and calculate the range of final gain levels that can be expected. It is not a purpose of this report to assign or predict these mechanical results, but only to direct attention to their final effect.

The rms surface error ϵ is expected to be as good as 0.5mm and no worse than 1.0mm. Using the Ruze formula, the resulting efficiencies may be as follows:

	Surface efficiency	
ϵ (mm), rms	8.45 GHz	2.295 GHz
1.0	0.8822	0.9908
0.5	0.9692	0.9977

Area blockage due to the feed support spars (quadripod) is expected to be between 6% and 8%. From JPL experience, the final blockage efficiency will be as follows, using

$$\eta \text{ (spar blockage)} = (1 - 1.2(Ap))^2$$

with Ap representing the geometric shadowing percentage by the spars.

Fractional area blocked	η (spar blockage)
0.06	0.861
0.08	0.817

When applying these extremes to the previously determined values of RF performance, the final gain results will be as tabulated in Table 3.

A most significant result to note is that X-band performance may improve almost a full decibel by careful engineering design of a best surface tolerance and minimum quadripod blockage. The design is seen to yield 68% X-band aperture efficiency within the very low noise design constraint under best conditions while providing simultanous 66% S-band efficiency.

References

1. Jeuken, E. J., and Vokurka, V. J., "Multi-Frequency Band Corrugated Conical Horn Antenna," *1973 European Microwave Conference Proceedings*, Vol. 2, Brussels University, Brussels, Belgium, Sept. 4-7, 1973.

2. Williams, W. F., "A Prototype DSN X-S Band Feed: DSS 13 First Application Status," *DSN Progress Report 42-44*, Jet Propulsion Laboratory, Pasadena, Calif., pp. 98-103, Apr. 15, 1978.

3. Williams, W. F., "DSN 100-Meter X- and S-Band Microwave Antenna Design and Performance," Publication, 78-65, Jet Propulsion Laboratory, Pasadena, Calif., pp. 13-14, Aug. 1978.

4. Williams, W. F., "A Prototype DSN X- and S-Band Feed: DSS 13 Application Status (Second Report)," *DSN Progress Report 42-47*, Jet Propulsion Laboratory, Pasadena, Calif., pp. 39-50, Oct. 15, 1978.

5. United States Patent No. 4199764, "Dual Band Combiner for Horn Antenna," Apr. 22, 1980, W. F. Williams and Seymour B. Cohn.

6. Thomas, B. Mac A., and Minnett, H. C., "Propagation in Cylindrical Waveguides with Anisotropic Walls," Publication RPP 1346, Division of Radiophysics, CS1RO, Sydney, Australia, Jan., 1977, also in *IEEE Transactions*, AP, Mar. 1978.

7. Williams, W. F., and Withington, J. R., "A Common Aperture S- and X-band Feed for the Deep Space Network," presented at the 1979 Antenna Applications Symposium, U. of Ill., Allerton Park, Sept. 1979.

8. Williams, W. F., and Reilly, H., "A Prototype DSN X/S Band Feed: DSS 13 Application Status (Fourth Report," *TDA Progress Report 42-60*, Jet Propulsion Laboratory, Pasadena, Calif., pp. 77-78, Dec. 15, 1980.

9. Williams, W. F., "LAAS Studies: 26-, 34-, and 40-Meter Elements," *DSN Progress Report 42-51*, Jet Propulsion Laboratory, Pasadena, Calif., p. 158, June 15, 1979.

10. Withington, J. R., and Williams, W. F., "A Common Aperture X- and S-band Four Function Feedhorn," presented at the 1981 Antenna Applications Symposium, University of Illinois, Allerton, Park, Sept. 1980.

Table 1. Final RF efficiency

	8.450 GHz	7.150 GHz	2.295 GHz	2.110 GHz
Rear spillover efficiency η_{rs}	0.9982 (0.4 K)	0.9970	0.9746 (6.1 K)	0.9695
Fwd. spillover efficiency η_{fs}	0.9839	0.9744	0.9100	0.9034
Illumination efficiency η_i	0.9823	0.9781	0.9874	0.9849
Cross-Pol. efficiency η_x	0.9988	0.9990	0.9995	0.9994
Phase efficiency η_{ph}	0.9744	0.9693	0.9383[a]	0.9593[a]
Cent. blockage efficiency η_{cb}	0.9826	0.9815	0.9765	0.9767
Dissipation, VSWR efficiency η_d	0.9700	0.9700	0.9700	0.9700
Total RF efficiency η	0.8949	0.8760	0.7779	0.7835

NOTE: Notice that no surface tolerance efficiency or quadripod blockage efficiency has yet been assigned.

[a]S-band phase center does not coincide with 8.450-GHz phase center, resulting in somewhat poorer phase efficiency at S-band. (Horn location and shaping are based upon the 8.450 GHz phase center.) 2.110-GHz phase efficiency calculates greater than 2.295 GHz because of slight differences in the scattered diffraction pattern.

Table 2. G/T calculations at 8.45 GHz

θ_2 illumination angle, deg	Total RF efficiency	Noise, rear, K (a) Zenith (b) 30° elevation	*Final $T(op)$, K (a) Zenith (b) 30% elevation	G/T, dB	Notes
70.78°	0.8872	(a) 7.54 (b) 3.77	25.04 26.37	55.06 54.84	$\theta_1 = \theta_2$
71°	0.8936	(a) 7.11 (b) 3.55	24.61 26.15	55.17 54.90	
71.949°	0.9052	(a) 1.8 (b) 0.9	19.30 23.50	56.28 55.42	θ_2 for maximum gain
72°	0.9052	(a) 1.6 (b) 0.8	19.10 23.40	56.32 55.44	
72.79°	0.8949	(a) 0.43 (b) 0.22	17.93 22.82	56.55 55.50	Maximum G/T for this antenna
73°	0.8908	(a) 0.25 (b) 0.12	17.75 22.72	56.57 55.50	
74°	0.8648	(a) 0.083 (b) 0.042	17.58 22.64	56.49 55.39	

[a]Total operating noise temp., neglecting rear spillover, is taken as 17.5 K for zenith and 22.6 K at 30° elevation.

Table 3. Final performance estimation

	8.450 GHz efficiencies		2.295 GHz efficiencies	
	max	min	max	min
RF efficiency	0.8949		0.7779	
Spar blockage efficiency	0.861	0.817	0.861	0.817
Surface efficiency	0.9692	0.8822	0.9977	0.9908
Total efficiency	0.7468	0.6450	0.6682	0.6297
Resulting gain limits, dB	68.30	67.66	56.49	56.24

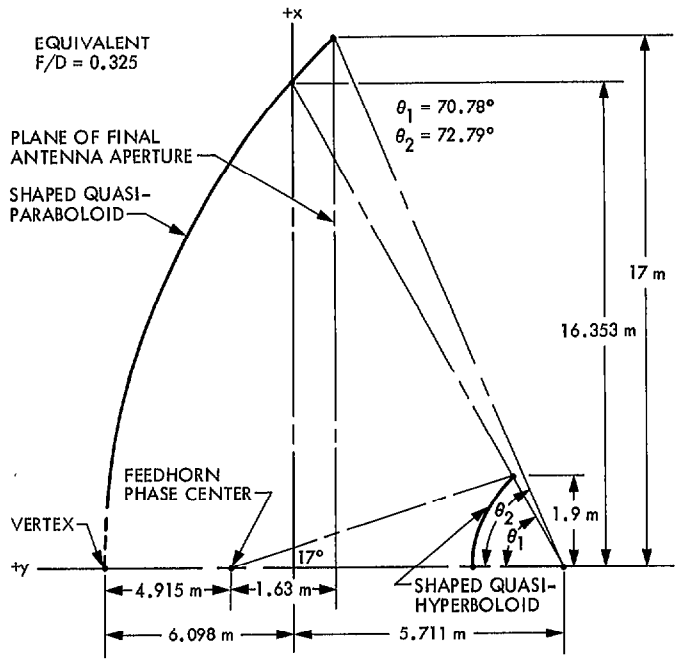

Fig. 1. Design control specification

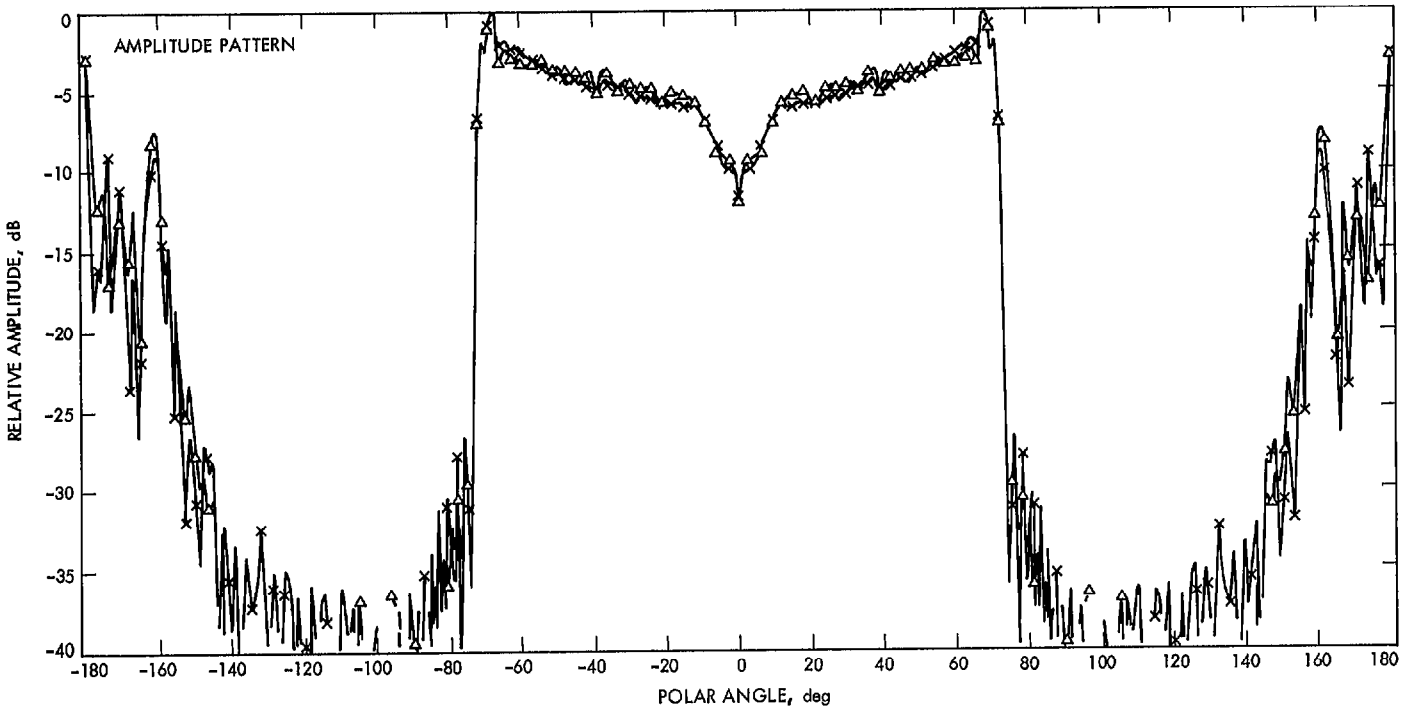

Fig. 2. Shaped subreflector scattering. Mod 2 X/S horn at 8450 MHz scattered from a 34-meter shaped subreflector

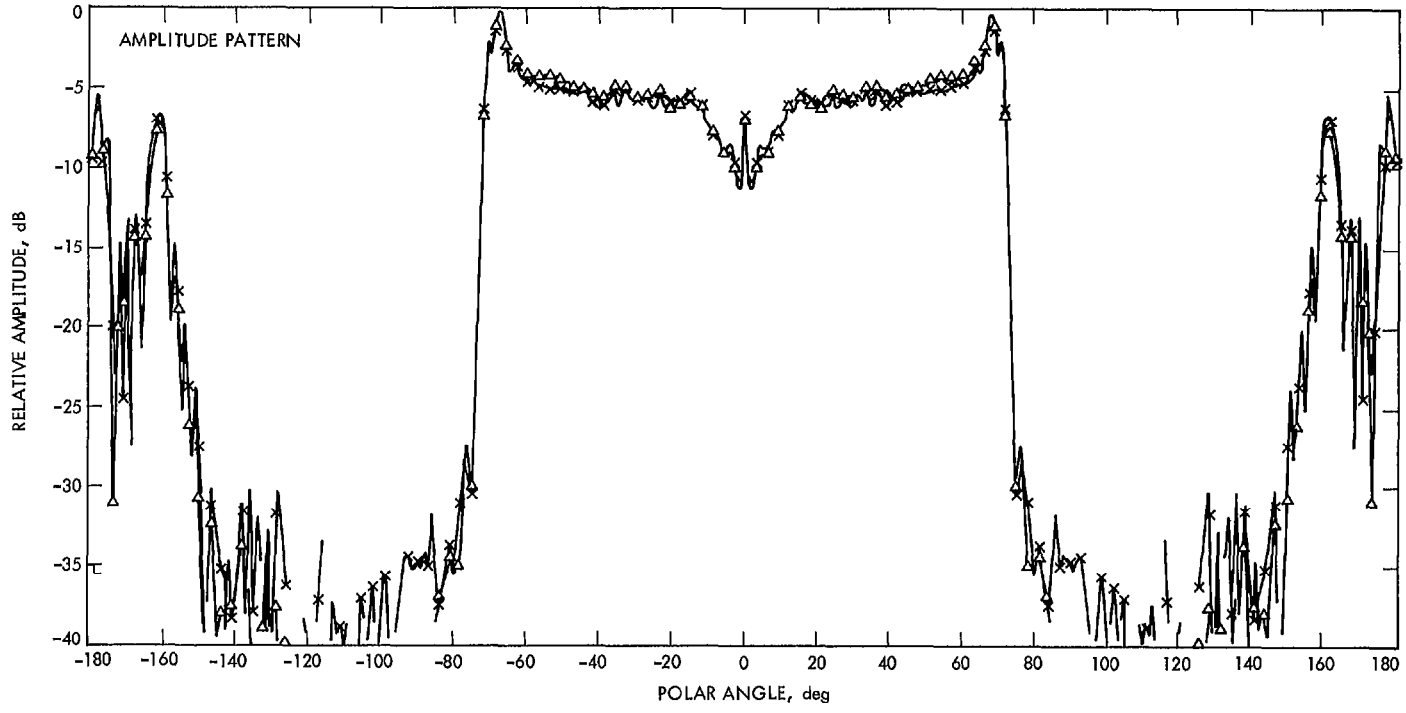

Fig. 3. Shaped subreflector scattering. Mod 2 X/S horn at 7150 MHz scattered from a 34-meter shaped subreflector

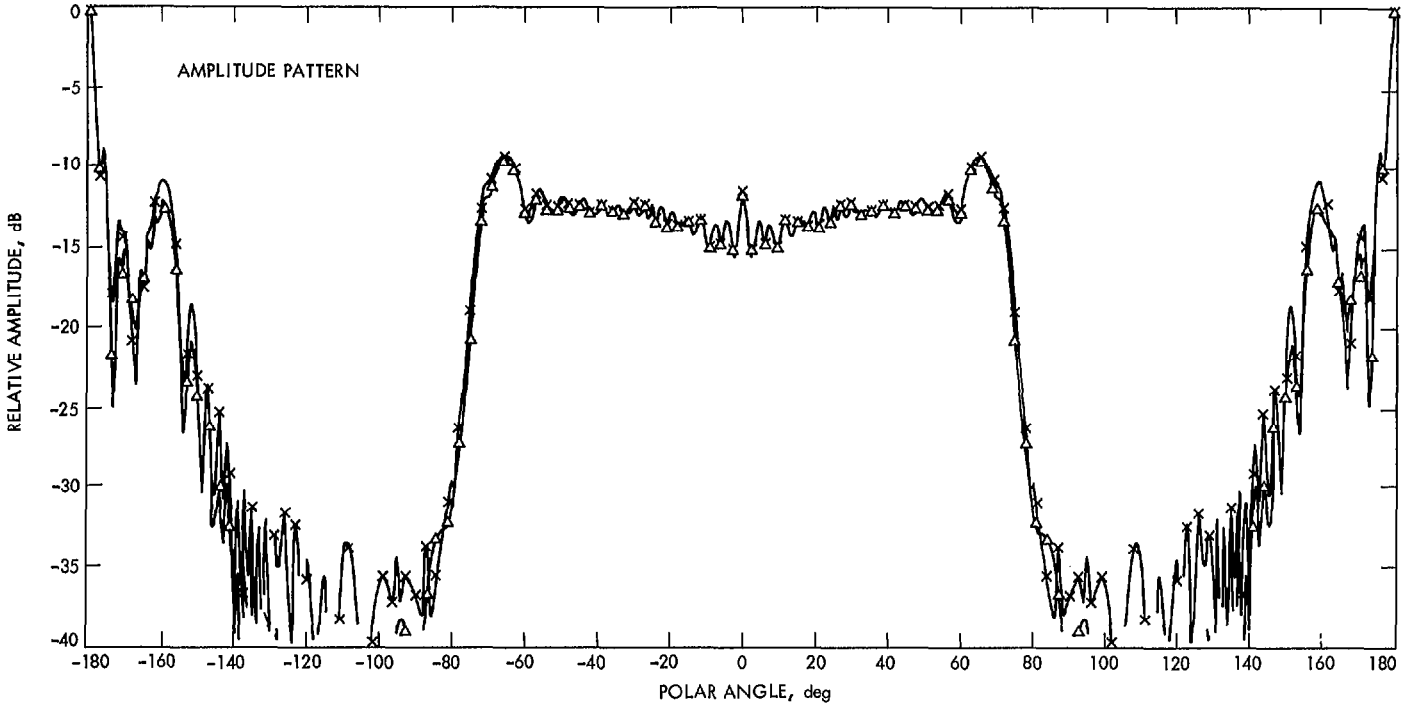

Fig. 4. A subreflector scattered pattern. Mod 2 X/S horn at 2295 MHz scattered from a 34-meter shaped subreflector

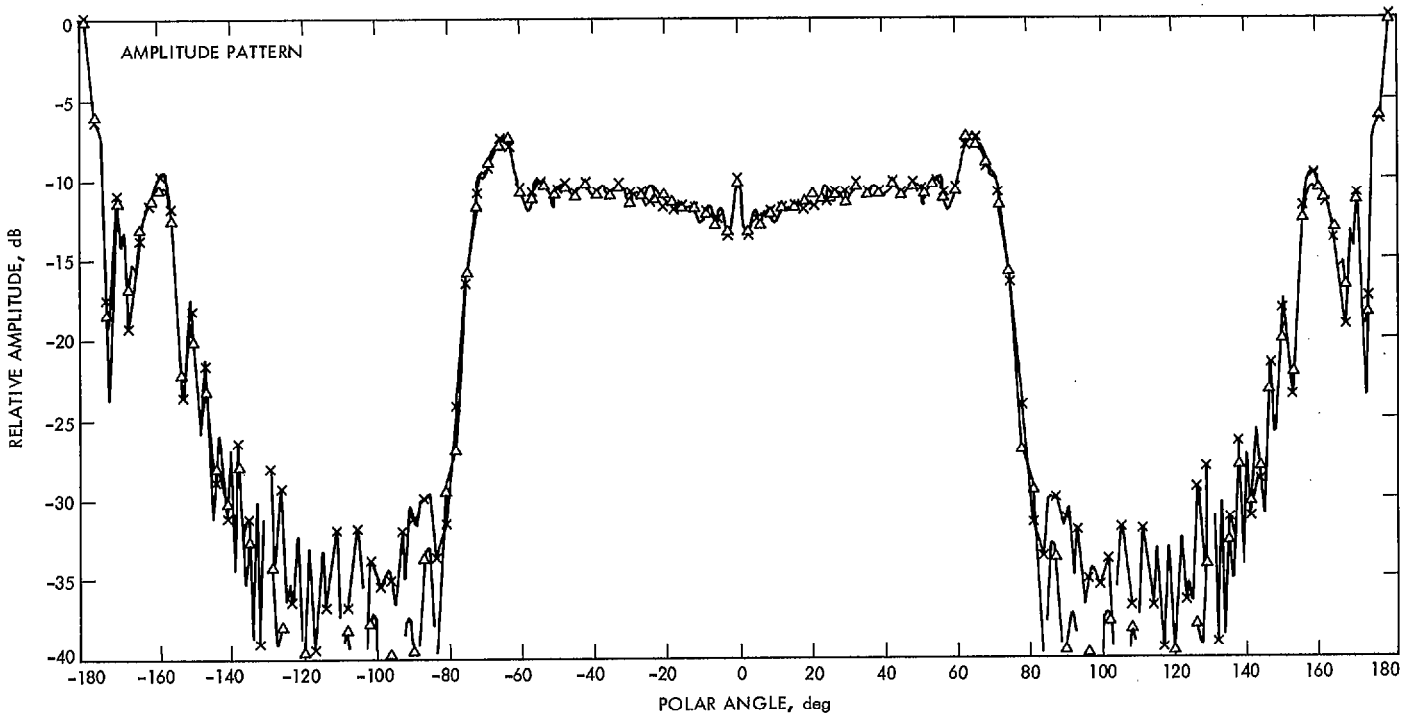

Fig. 5. Subreflector scattering. Mod 2 X/S horn at 2110 MHz scattered from a 34-meter shaped subreflector

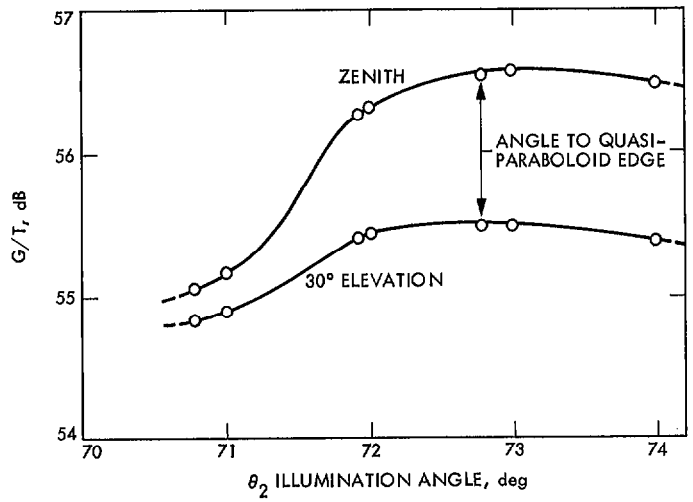

Fig. 6. G/T of system vs edge illumination angle

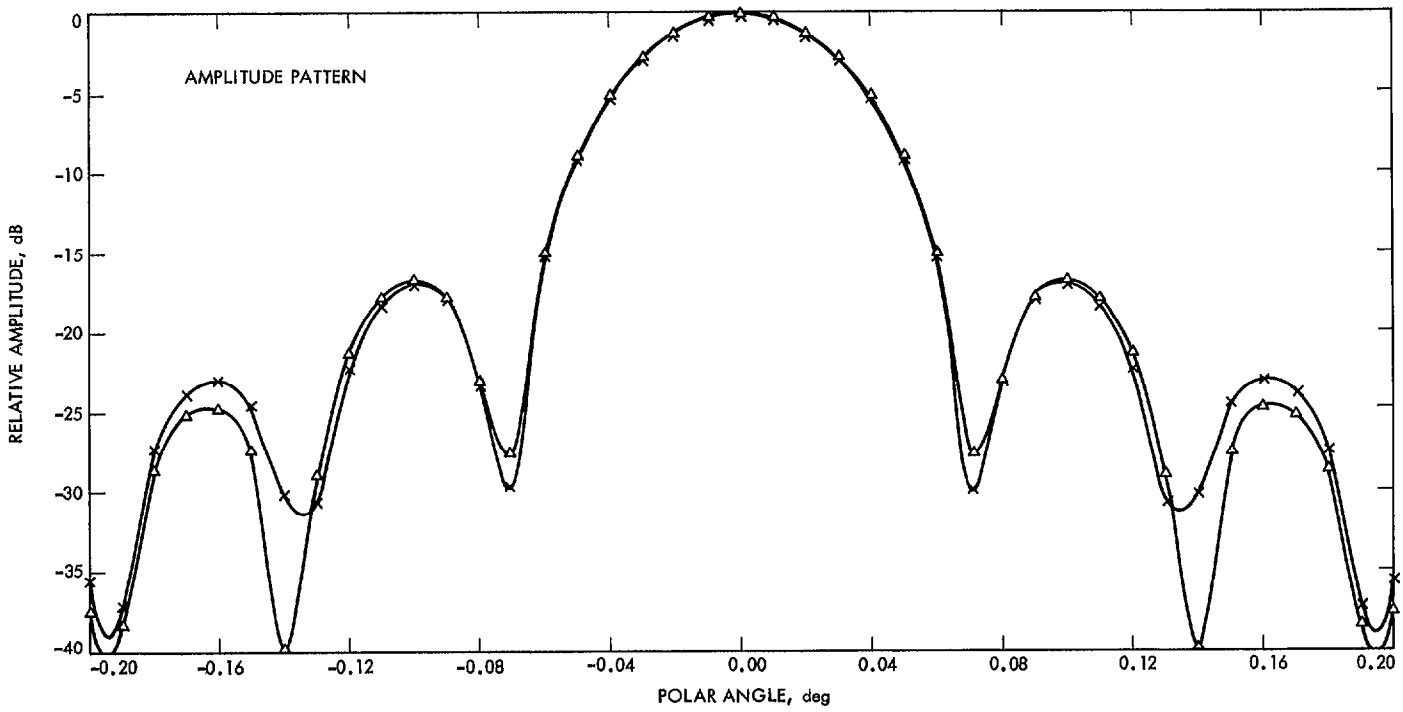

Fig. 7. Secondary pattern scattering. The 8450-MHz real cassegrain pattern after phase correction. Scattered from the equivalent 34-meter paraboloid. F = 454 inches, giving the proper illumination

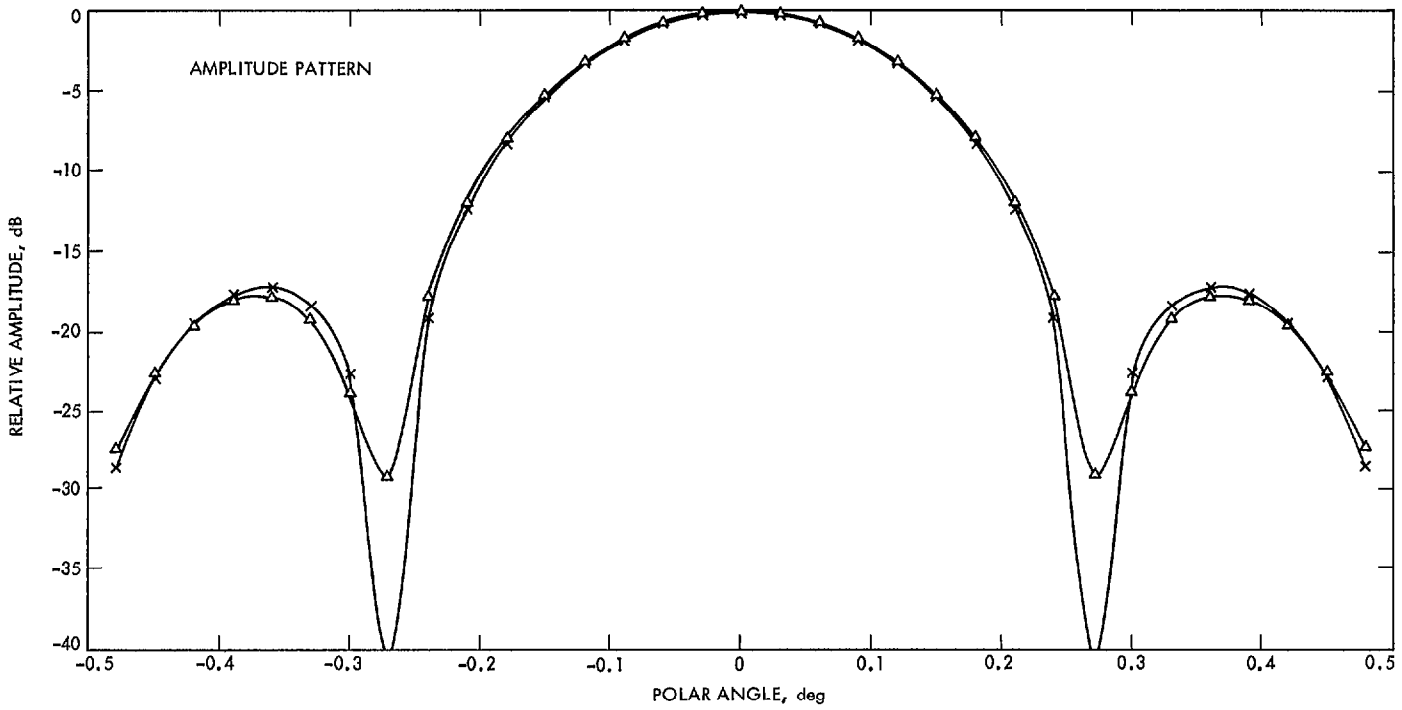

Fig. 8. Secondary pattern scattering. The 2295-MHz real cassegrain pattern after phase correction. Scattered from the equivalent 34-meter paraboloid. F = 454 inches, giving the proper illumination